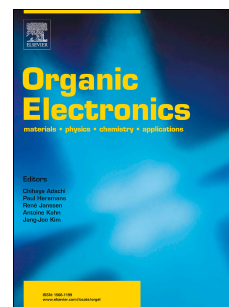# Journal Pre-proof

Analysis and simulation of reddish overshoot in active matrix organic light-emitting diode display with varying p-doped hole transport layer concentrations

Jung-Min Lee, Chang Heon Kang, Juhn Suk Yoo, Han Wook Hwang, Soon kwang Hong, Yong Min Ha, Byeong-Kwon Ju
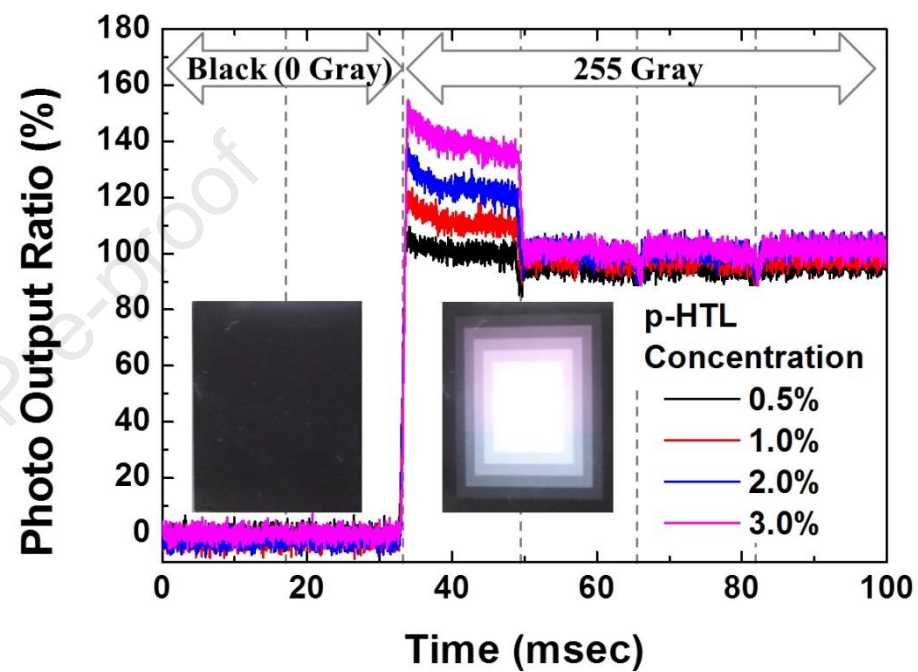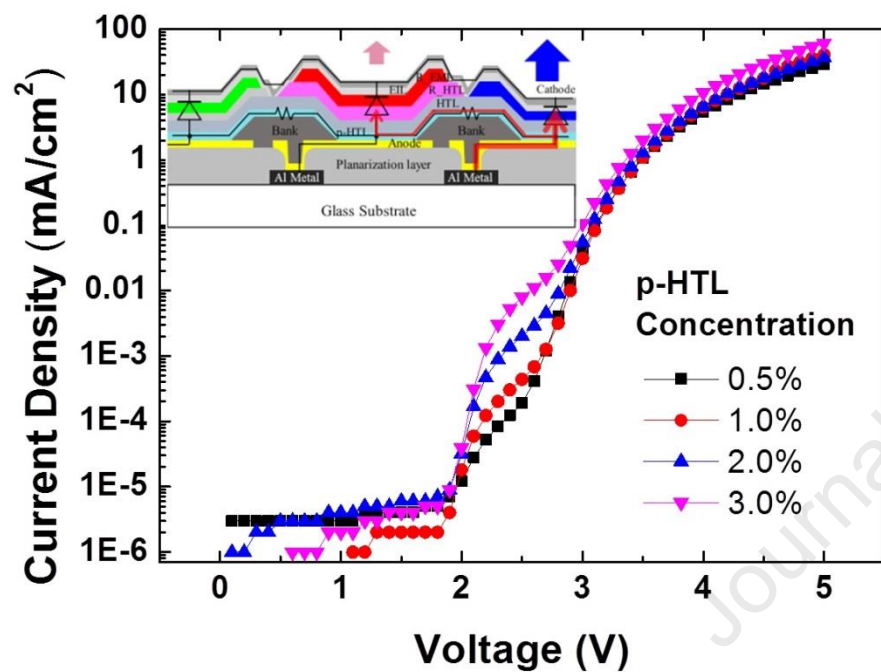
Please cite this article as: J.-M. Lee, C.H. Kang, J.S. Yoo, H.W. Hwang, S.k. Hong, Y.M. Ha, B.-K. Ju, Analysis and simulation of reddish overshoot in active matrix organic light-emitting diode display with varying p-doped hole transport layer concentrations, *Organic Electronics* (2021), doi: https://doi.org/10.1016/j.orgel.2021.106328.

This is a PDF file of an article that has undergone enhancements after acceptance, such as the addition of a cover page and metadata, and formatting for readability, but it is not yet the definitive version of record. This version will undergo additional copyediting, typesetting and review before it is published in its final form, but we are providing this version to give early visibility of the article. Please note that, during the production process, errors may be discovered which could affect the content, and all legal disclaimers that apply to the journal pertain.

Graphical Abstract

Analysis and simulation of reddish overshoot in active matrix organic light-emitting diode display with varying p-doped hole transport layer concentrations

Jung-Min Lee[a,b], Chang Heon Kang[b], Juhn Suk Yoo[b], Han Wook Hwang[b], Soon kwang Hong[b], Yong Min Ha[b] and Byeong-Kwon Ju[a,*]

[a] Display and Nanosystem Laboratory, Department of Electrical Engineering, Korea University, Seoul 02841, Republic of Korea

[b] LG Display Co., Ltd., Paju 10845, Gyeonggi-do, Republic of Korea

*Corresponding author: Prof. Byeong-Kwon Ju

Email: bkju@korea.ac.kr

Laboratory Homepage: http://diana.korea.ac.kr

Tel.: +82-(0)2-3290-3671, Fax: +82-(0)2-3290-3791

Abstract

A typical organic light-emitting diode (OLED) display has common organic layers between adjacent pixels, which ensure ease of manufacturing process and efficiency in operation. The p-doped hole transport layer (p-HTL) has low electrical resistivity, which results in a high efficiency OLED. However, the low resistivity results in various side effects, including color crosstalk and overshoot, mainly due to lateral leakage current flowing through this layer. Furthermore, virtual reality and augmented reality devices that require extremely high pixels per inch (PPI) and superior image quality are very sensitive to lateral leakage current. In this study, we propose a passive driving panel based on RGB top emission to efficiently measure and model the lateral leakage current characteristics according to the p-HTL concentration.

In addition, we constructed a 1.5-inch active matrix organic light-emitting diode panel based on the n-type low-temperature polycrystalline silicon 4T2C pixel circuit. Subsequently, we quantitatively analyzed the reddish overshoot phenomenon during the black to white image transition. This effect was reduced at p-HTL concentrations under 1%.
Finally, we analyzed the overshoot mechanism through SPICE simulations and realized the optimal lateral resistance value of the common organic layer for each PPI.

Keywords

lateral leakage current, p-doped hole transport layer, active matrix organic light-emitting diode, overshoot, SPICE simulation

1. Introduction

Over the past few decades, the organic light-emitting diode (OLED) technology has made tremendous progress, owing to its exceptional characteristics, such as wide color gamut, fast response time, high contrast ratio, and wide viewing angle [1–3]. OLED displays are rapidly replacing liquid crystal displays in mobile devices as well as televisions. The use of OLED is not just limited to the aforementioned applications; they are widely used in wearable, automotive, and virtual reality (VR) devices because of their flexible and free form display capabilities [4–6].

The pixel structures for commercial OLED displays can be configured with two primary methods—white and RGB OLEDs [7,8]. Both methods include common layers in hole transport layer (HTL), electron transport layer (ETL), and cathode to ensure simplicity in manufacturing and mass productivity. The only exception is the separate deposition of the emissive layer (EML) using patterned fine metal mask (FMM) from the RGB OLED. The p-doped HTL (p-HTL) among the common layers yields high efficiency because it improves the carrier injection to the HTL and facilitates sufficient conductivity [9–11]. Although most OLED pixel currents flow vertically toward the cathode, the lateral leakage current flows to neighboring pixels through the p-HTL with high conductivity [12]. This could potentially alter the original current-voltage characteristics and result in color crosstalk and gamma distortion, thereby hampering the display quality [13,14].

The pixel current required to achieve target luminance has decreased for modern displays; the primary focus of modern displays is to achieve a high current efficiency of over 100 cd/A and pixel density of more than 5000 pixels per inch (PPI) [15,16]. Therefore, the lateral leakage current has a more significant effect on the image quality.

Previous studies were mainly focused on static operations at the device level for lateral leakage current. Furthermore, to the best of our knowledge, dynamic behaviors such as response characteristics have not been reported at the system level yet. Fig. 1 shows the still

images converted from black to gray pattern on an active matrix organic light-emitting diode (AMOLED) panel designed in this study; the images were captured using a high-speed camera. In the first frame, the image turns reddish and brighter and returns to the original image from the second frame. This reddish overshoot phenomenon causes a motion blur when the images or texts are scrolled over a black background. Moreover, for a VR display that requires fast response speed, the aforementioned problem becomes more apparent.

  In this study, we investigate the effect of the lateral leakage current on the AMOLED display according to the p-HTL concentration. First, the passive driving panel of the RGB top emission type was constructed to accurately measure and model the lateral current characteristics of the OLED. We quantitatively analyzed the overshoot phenomenon by constructing a 1.5-in AMOLED panel based on an n-type low-temperature polycrystalline silicon (LTPS) 4T2C pixel circuit, which has superior V_{th} compensation ability. The results of simulation program with integrated circuit emphasis (SPICE) in a new OLED model demonstrate the reddish overshoot mechanism and yield the optimal lateral resistance value of the common organic layer for each PPI.
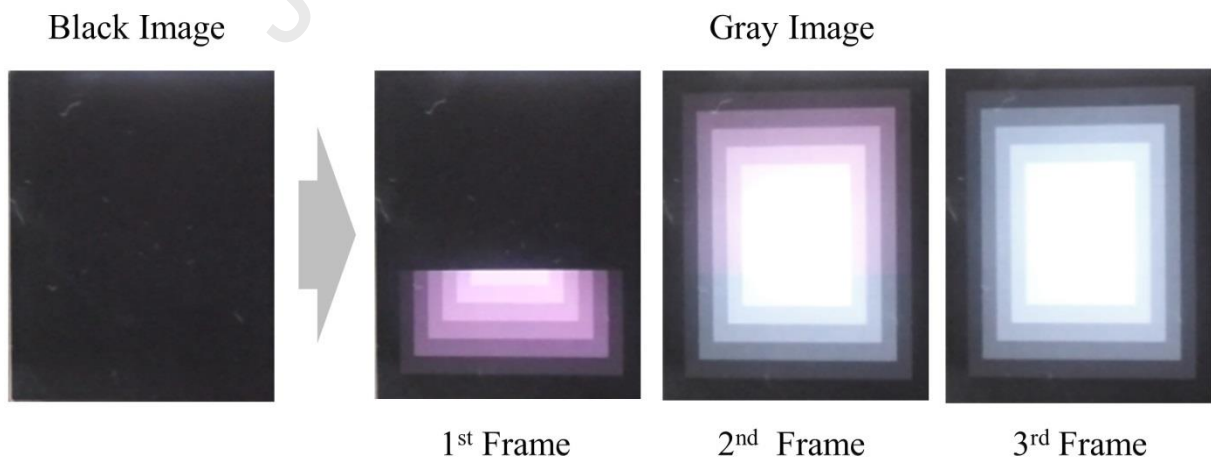

Fig. 1. Still images captured using a high-speed camera

2. Experiments

A passive driving panel with the same pixel structure as an AMOLED panel was manufactured to measure the lateral leakage current and current density-voltage-luminescence (J-V-L) characteristics of the RGB OLED. Fig. 2(a) shows a panel layout and fabricated RGB modified stripe pixel configuration with a 78 µm pitch for a high aperture ratio. The emission area of each RGB pixel is 20.5×8.0, 20.5×10, and 9.5×53.5 µm^2; the average aperture ratio is 14.4%.

Although the panel size was 1.5 in, the luminous area was set at 18.02×12.48 mm^2 to minimize the luminance imbalance caused by the voltage drop (IR drop). The anode is connected separately to turn on RGB individually, and the cathode is connected in common, as shown in Fig. 2(b).
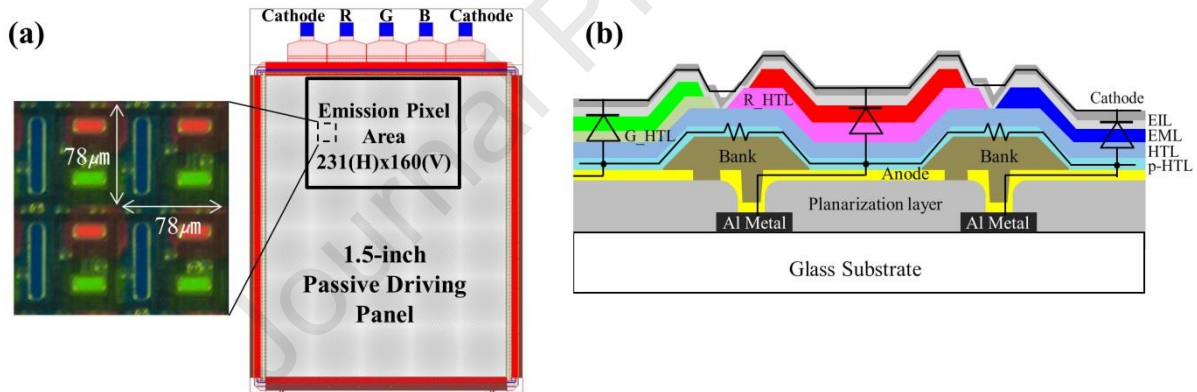
Fig. 2. (a) Optical photograph of fabricated pixels and panel layout of passive driving RGB OLED with 326 PPI

(b) Cross sectional view of RGB OLED layer structure

The EMLs, R′ and G′ HTL for microcavity control is deposited separately on each RGB sub-pixel using patterned FMM. Other layers such as p-HTL, HTL, ETL, and cathode are deposited uniformly using a common shadow mask. In addition, an AMOLED panel with a 4T2C pixel circuit was constructed using the NMOS LTPS thin-film transistor (TFT) process to analyze the effects of lateral leakage current in the dynamic operational state of the display.

The motion blur phenomenon of the display was measured using a high-speed camera (Photron UX50). The OLED characteristics and lateral leakage current were tested with a Keithley 2400 source meter connected to a spectroradiometer (Photo Research Spectra Scan PR-655). The luminance response characteristics of the AMOLED were measured using a digital oscilloscope (Tektronix TDS2000C) and a photosensor amplifier (Hamamatsu C6386-01). The color coordinate variations during the transition of images of AMOLED were measured using a display color analyzer (Minolta CA310). We performed a pixel circuit simulation using Smartspice and OLED models extracted by UTMOST IV from Silvaco Inc.

3. Results and discussion

3.1 OLED characteristics
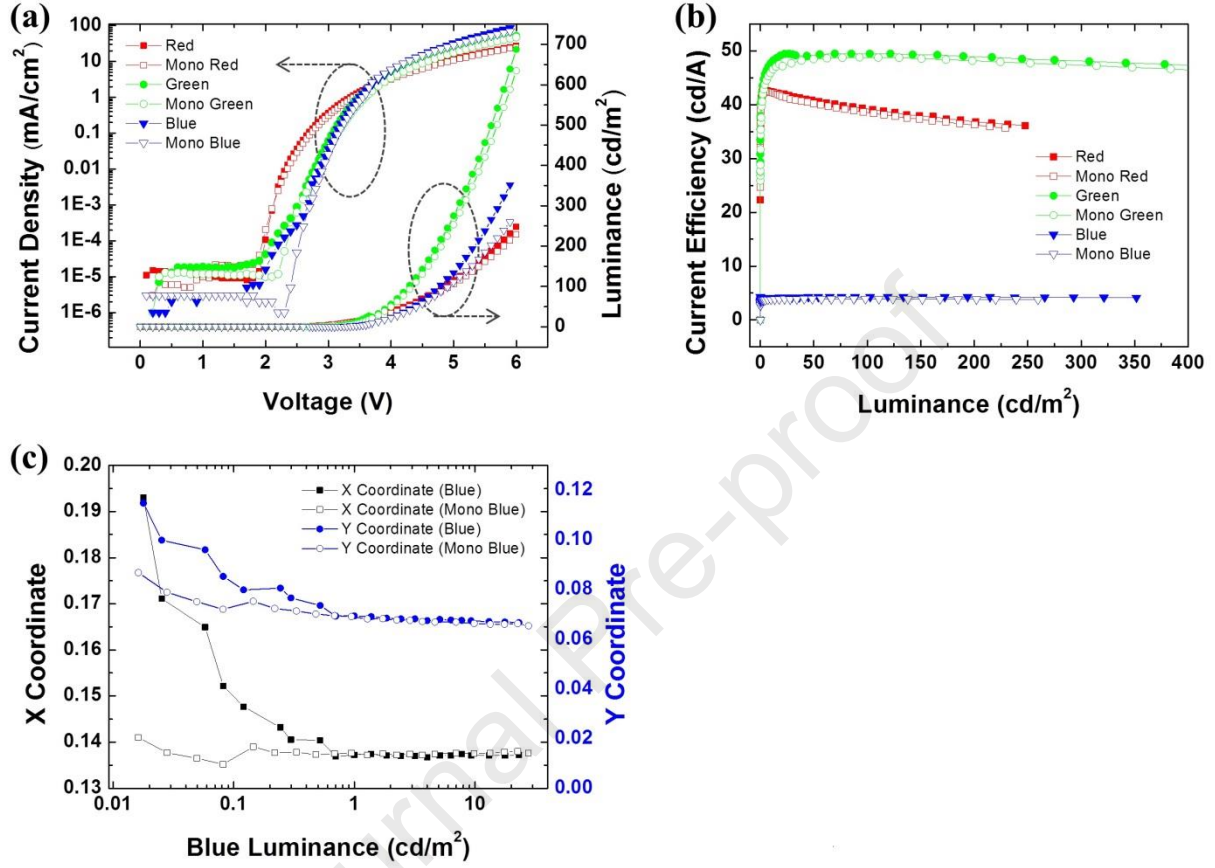
Fig. 3. Electro luminescence characteristics of RGB and mono color panel. (a) Current density and luminance with respect to voltage (b) Current efficiency with respect to luminance (c) CIE color coordinate of blue OLED with luminance

Table 1. Characteristics of RGB OLEDs of the fabricated passive driving panel at 100 cd/m^2

	Current Efficiency [cd/A]	Voltage (V)	Turn on voltage(V)[a]	CIE Coordinate (x)[a]	CIE Coordinate (y)[a]
Red / Mono Red	39.1 / 38.9	4.9 / 4.9	2.2 / 2.2	0.662 / 0.664	0.328 / 0.329
Green / Mono Green	49.5 / 48.8	4.3 / 4.3	2.65 / 2.7	0.293 / 0.284	0.612 / 0.617
Blue / Mono Blue	4.2 / 3.9	4.9 / 5.0	2.75 / 2.9	0.171 / 0.137	0.099 / 0.078

a) at 0.02 cd/m^2

To study the effect of the lateral leakage current flowing through a common layer and the characteristics of OLEDs with a p-HTL concentration of 2%, we fabricated a color panel with an RGB OLED and a mono panel with only a single color. The RGB electro luminescence characteristics of the fabricated OLED panel are presented in Fig. 3 and Table 1. The fabricated phosphorescent red OLED exhibited the lowest turn-on voltage of 2.2 V, while the fluorescent green and blue OLEDs exhibited turn-on voltages of 2.7 and 2.9 V, respectively. The electro-optical properties of RGB OLEDs indicate that they suffice the implementation of high luminance AMOLED displays over 600 nit. All OLEDs with the same color exhibited almost identical current density, voltage, and efficiency characteristics above 100 cd/m^2. However, increased current efficiency and current pump characteristic near the turn-on voltage of the blue OLED were observed, as compared to the mono blue OLED, which is shown in Figs. 3a and 3b. The turn-on voltage of the blue OLED also decreased by 0.15 V. After studying change in x and y coordinates due to the blue luminance in Fig. 3(c), it can be inferred that on decreasing the luminance, the x and y coordinates increased in the blue OLED compared to that of the mono blue OLED, and a similar color shift was also observed in the green OLED (Table 1).

It is expected that the red OLED is turned on at the same time as the lateral leakage current, when the voltage is applied to the blue or green OLED. This is because the red OLED required the lowest turn-on voltage and relatively high current efficiency. In addition, measuring the characteristics of a mono OLED without the interaction with RGB OLEDs is important for accurate modeling. Fig. 4 shows the current density−voltage curve of the blue OLED, and the current-voltage characteristics of the blue and red anodes in the floating state of the cathode according to the p-HTL concentration. The current pump characteristics in the turn-on voltage area of the blue OLED was enhanced by increasing the p-HTL concentration from 0.5 to 3.0% because of the high lateral leakage current, as shown in Fig. 4(a). This

makes it difficult to obtain the characteristics of the original device as the influence of the neighboring pixels grows; it creates image distortions such as color crosstalk. Similar studies and attempts to resolve this problem from a structural perspective of devices have been reported [17–19]. But these technologies are difficult to apply to display industry because they require the introduction of completely new equipment, processes and materials. Although pattering technology using FMM is a good way to mitigate this problem, it could not fully remove the overlapping organic layers between pixels due to shadow effect [20].

The lateral sheet resistance (R_{sheet_pxl}) between sub-pixels can be obtained from the result of Fig. 4(b). and the results calculated by Eq. (1) are presented in Table 2.

$$R_{sheet\_pxl} = \frac{Voltage}{I_{panel}/PXL_{num}} \times \frac{W_{com}}{L_{com}} \qquad (1)$$

where PXL_{num} (231 × 160 ea) is the number of emission pixels, I_{panel} is the current between anodes, and L_{com} (24 µm) and W_{com} (8 µm) are the length and width of the organic common layer between blue and red pixels, respectively. The sheet resistance of the common layer between the red and blue pixels decreased exponentially from 245 to 5.5 $G\Omega$/sq. as the doping concentration increased from 0.5 to 3.0%, mainly due to improved carrier injection properties.
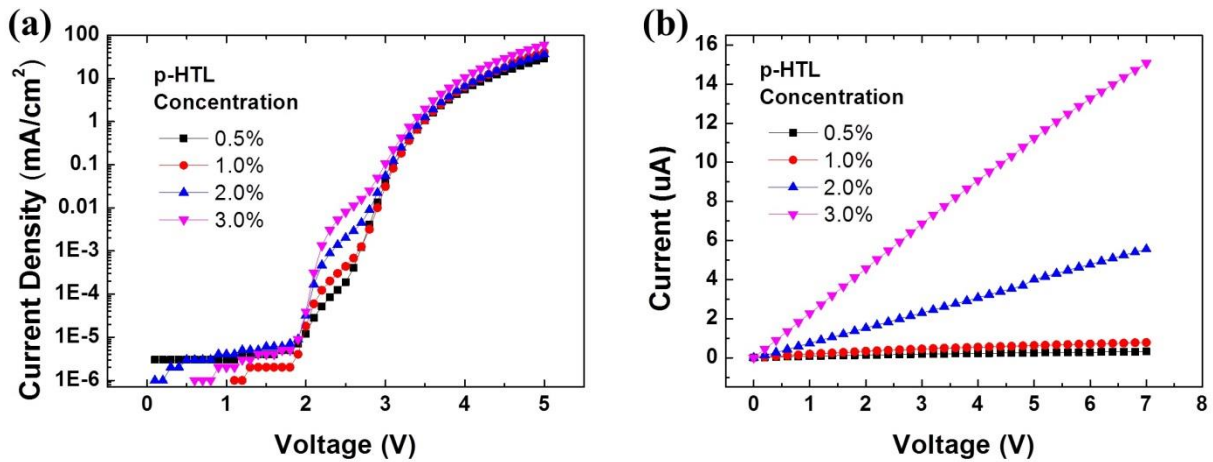

Fig. 4. Blue OLED characteristics of color panel according to p-HTL concentration (a) Current density-voltage curve (b) Current-voltage characteristic between blue and red anode

Table 2. Lateral sheet resistance of the fabricated panel

p-HTL Concentration	0.5%	1.0%	2.0%	3.0%
I_{panel} (μA)	0.251	0.623	2.0	11.2
R_{sheet_pxl} ($\Omega/sq.$)	2.45E+11	9.89E+10	1.54E+10	5.50E+9

3.2 AMOLED transient characteristics

We analyzed the correlation between the reddish overshoot phenomenon and p-HTL concentration of the AMOLED, as shown in Fig. 1. Various factors such as response time, uniformity, crosstalk, contrast ratio, and residual image depend heavily on the backplane and compensation pixel circuit in the AMOLED display [21–24]. The n-type LTPS 4T2C pixel circuit was selected because of its excellent TFT threshold voltage (V_{th}) compensation performance and the reliability of the backplane in this evaluation. The detailed description of the operation of the pixel circuit is specified in a previous paper [25], Fig. S2 and Table S2. Fig. 5(a) shows the RGB OLED response characteristics with p-HTL concentration of 2%, when changing from black to white (255 gray level) measured in the photodiode. On this AMOLED, a frame time of 16.6 ms and a horizontal line time of 37 μs were recorded. If the AMOLED has an ideal response characteristic, all RGBs should maintain a constant shooting amount ratio (SAR) from the first frame when changing to 255 gray. SAR is the ratio of the peak photo intensity between the first frame (A1) and the frame with a stable luminance (A3). The positive and negative values indicate overshoot and undershoot, respectively. The SARs of the RGB are 29%, 5%, and 2%, respectively, which match well with the reddish phenomenon in the gray pattern in Fig. 1.
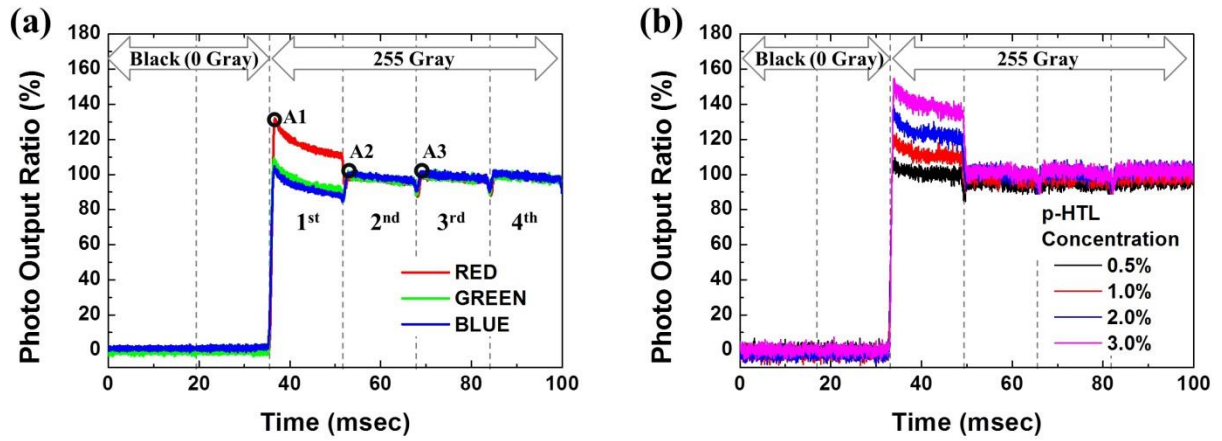
Fig. 5. (a) Response characteristics of RGB OLEDs when converted from black (0 Gray) to white (255 Gray) (b) Response characteristics of red OLED according to the p-HTL concentration

This reddish overshoot causes a perceived motion picture blur while scrolling images or text on a black background owing to the difference in luminance and color among frames. Fig. 5(b) shows the response characteristics of red pixels with varied p-HTL concentrations. When the doping concentration was reduced to either 1.0 or 0.5%, the overshoot phenomenon of the red OLED was significantly reduced. The SARs of red OLED were 6%, 16%, 32%, and 51% and doping concentrations were 0.5%, 1.0%, 2.0%, and 3.0%, respectively. It can be inferred from these experimental results that there is a significant correlation between the lateral leakage current and the red overshoot phenomenon.

Fig. 6 shows the color coordinates of the AMOLED samples during the continuous transition of black and white images into one frame unit compared to the white image according to the p-HTL concentration. The color coordinates shifted to the reddish direction as the doping concentration increased, which is similar to the SAR results. The average x coordinate shift was 0.053, 0.045, 0.032, and 0.014 for p-HTL at 3%, 2%, 1%, and 0.5%, respectively. We quantitatively measured the color coordinate shift in the gray pattern using this method; this is because it is possible to continuously reproduce the red overshoot phenomenon by repeating black and white images. Although the existing response

characteristics were measured based solely on luminance variation [26,27], this method allows the measurement of changes in the color coordinates as well as luminance.
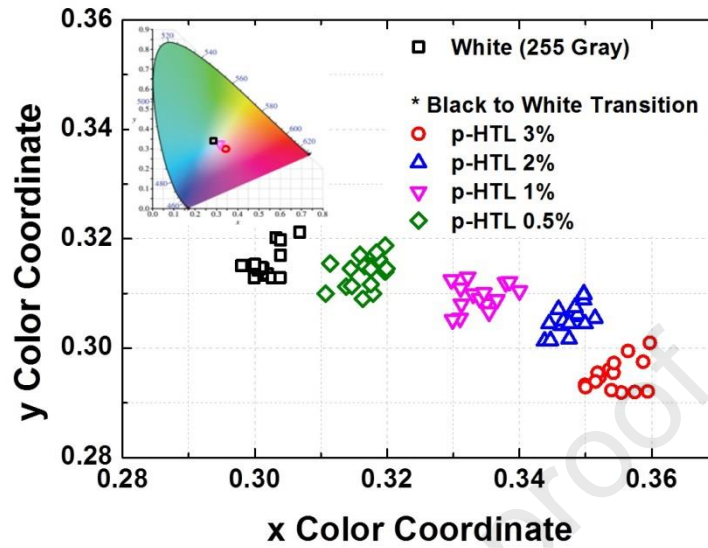

Fig. 6. Color coordinates during transition of black and white image in frame units compared to white image

3.3 OLED modeling

To analyze the reddish overshoot phenomenon, OLED modeling and SPICE simulations were conducted. OLED modeling is important for analyzing various image quality characteristics. Different types of models considering electrical, thermal, and optical characteristics as well as lifespan of OLEDs have been introduced [28–31]. We proceeded with OLED modeling by focusing on the electrical characteristics in this study. Fig. 7 shows the OLED model used for this simulation and the fitting current density−voltage curve of the blue OLED with measured lateral resistance. We used four diodes, D1−D4 (Diode model level 3) with a series voltage source V_1 for the V_{th} control connected in parallel with a capacitor C_{EL}, as shown in Fig. 7(a). To calculate the capacitance of the OLED, the relative permittivity of the organic layer is assumed as 2.0, with regard to the luminance area, thickness of organic layers, and parasitic cap. Therefore, the capacitance C for each RGB OLED is 16.4 fF, 25 fF, and 78.3 fF. Four diodes were used to accurately fit turn off, turn on,

middle current, and high current areas in the current density-voltage curve of each RGB

OLED, and lateral resistance was added between the R, B, B, and G anodes in to reflect the

hump characteristics in the turn-on area. SPICE parameters were extracted based on mono

RGB OLED measurement results using the modeling software UTMOST IV.

As shown in Fig. 7(b), with the obtained OLED model, an accurate fit between simulated and

measured device characteristics through the optimization of the SPICE model parameters, was

realized.
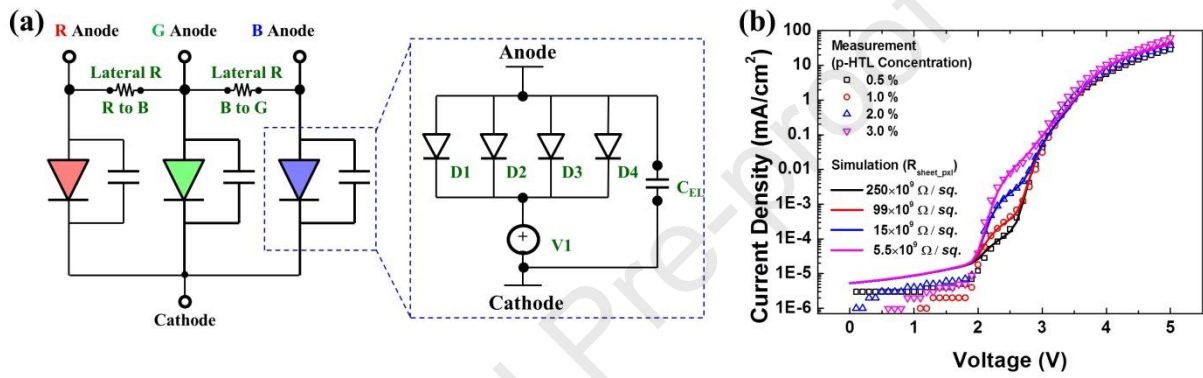
Fig. 7. (a) OLED model used for simulation (b) Modeled and measured current density-voltage curve of blue

OLED

3.4 Pixel simulation and discussion on improvement
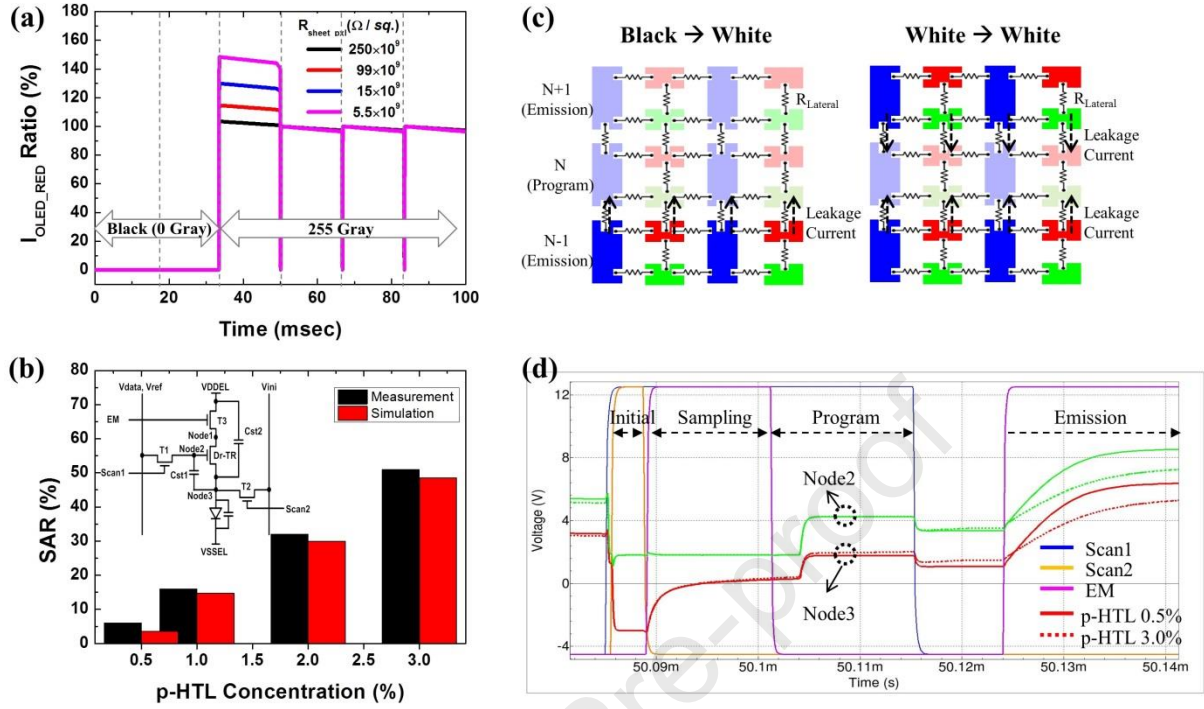
Fig. 8. (a) Simulated transient waveforms of OLED current of red pixel with different lateral sheet resistances (b) Red pixel SAR simulation and measurement results of AMOLED panel (inset)—Schematic of 4T2C pixel circuit (c) Conceptual image of current flow among anodes when switching from black to white and white to white

(d) Simulated transient waveform of node2, node3, and control signals for 0.5% and 3% p-HTL variation

Reduced 4×RGB×4 pixel block is used for efficient panel simulation as shown in Fig. S3. Peripheral circuits are consisted of control signal blocks, data and power signals. The chanel width and length of driving TFT are 3.5 µm and 20 µm. All switching TFTs are 3.5 µm of the chanel width and 4 µm of the length. For the pixel circuit VDDEL, VSSEL, Vref and Vini are 8.5, 0, 1.5, -5V, respectively. The Scan1, Scan2 and EM signals swing from 12.5 to -4.5V. The simulation and pixel design parameters are listed in Table S3.

Fig. 8(a) shows the simulated red OLED current ratio of the 4T2C pixel circuit with different lateral sheet resistances. As the lateral resistance reduces by 5.5 $G\Omega$, the overshoot phenomenon occurs significantly when switching from black to 255 Gray

(white), resulting in motion blur. Before the conversion with respect to the current ratio, the simulated pixel current waveform with low lateral resistance indicates that the overall current is also low. Compared to the SAR measurement results of the red pixel, the simulation is well matched with an error of approximately 3%, as shown in Fig. 8(b).

We believe that we can further improve this model if the schematic of the resistors connected in the form of mesh between the pixel anodes was configured accurately. The variations in the overall current and the red overshoot phenomena were caused by the lateral resistance, which is explained in Figs. 8(c) and (d). The operation of the 4T2C pixel circuit is divided into initial, sampling, and program for 1 horizontal line (1H) time; the remaining time is emission. Furthermore, node2 and node3 are the gate and source voltages of the driving TFT [inset Fig. 8(b)]; they play an important role in determining the pixel current.

Subsequently, node2 is maintained at a constant voltage of V_{ref} and V_{data} for 1H time, while node3 remains in a floating state at the end of the sampling and during the program period. Therefore, when switching from black to white, the node3 voltage is affected by the lateral leakage current from the pixels in the direction of the emitted light. The process of switching from white to white, is affected by the emission of the pixels in both directions, as shown in Fig. 8(c). In addition, the node3 voltage of red pixels increases the most due to the lateral leakage current because the red OLED has the smallest turn-on voltage and capacitance. The V_{gs} of the Dr-TFT decreases with the increase in node3 voltage, and the pixel current and luminance decrease as well. Fig. 8(d) shows that the node3 voltage increases due to the leakage current from the neighboring pixels when the lateral resistance is low, as explained above. As a result, the red overshoot phenomenon is multiplied by the resistance of the OLED common layer, the luminance state of neighboring pixels during pixel program operation, and the difference of turn-on voltage and capacitance among RGB OLEDs.

In this study, we obtained a lateral sheet resistance for optimal image quality through panel evaluation and simulation with 326 PPI AMOLED according to p-HTL concentration.

However, the pixel current required to achieve the specified luminance decreases with the increase in PPI, and the effect of the lateral leakage current affects the image quality more sensitively. Therefore, we propose the optimal lateral resistance value of the common organic layer for each PPI based on simulation results, as shown in Fig. 9.
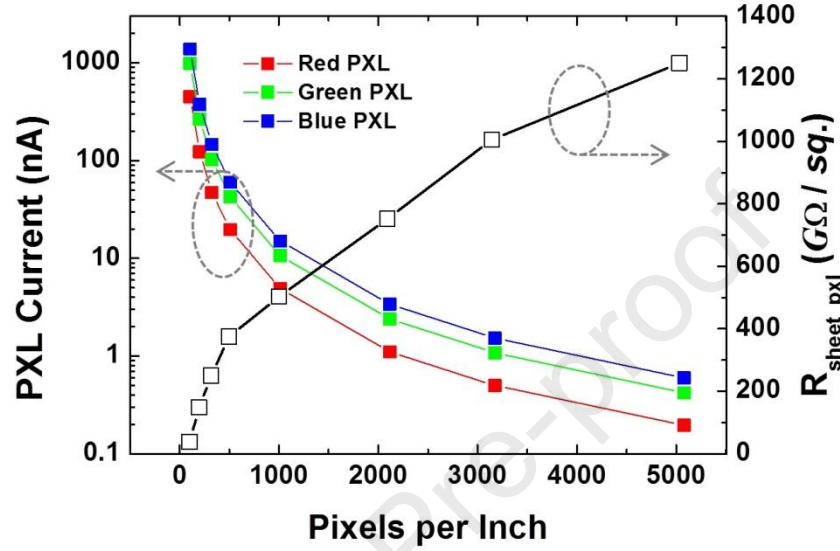
Fig. 9. Required RGB pixel current for white and lateral sheet resistance of OLED for optimal image quality with respect to PPI

The method of increasing lateral resistance for AMOLED displays of high PPIs should not be limited to material. This is mainly because efficient values of driving voltage, efficiency, and lateral resistance of OLEDs cannot be obtained only through material characteristics including doping control. Therefore, the research should extend to bring about improvements in the device structure and driving scheme as well. The overdrive is one of the most widely used technologies to improve transient reponse characteristics of AMOLED displays as well as active matrix liquid-crystal displays (AMLCDs). These studies showed the high motion image quality using overdrive technology with dithering algorithm and look-up table [32, 33]. However, we need advanced overdrive technology to improve the reddish overshoot phenomenon in various display operation and ambient temperautre conditions. The overdrive voltage applied to each RGB pixel should be adjusted individually for transient white color

balance. In addition, the optimized lookup tables are required to compensate temperature dependence of OLED characteristics and luminance deviation according to the data transition history of the previous frames.

The 4T2C pixel circuit used in this study has superior V_{th} compensation ability, but the node3 is affected by the lateral leakage current from the emitting neighboring pixels. The Vgs of the Dr-TFT is changed by node3 voltage, which affects transient image quality. Thus pixel circuit can be improved further by new driving scheme which has non emitting hold period of upper and lower pixels during the program period. We can expect the RGB colors balance during the transient frame by minimizing the lateral leakage current.

Another strucrual improvement of the OLED is to add the reverse spacer on the bank, which can block the connections between adjacent pixels and common organic layer without using FMM. This is similar structure with cathode seperator for passive matrix OLED [34]. However, reverse spacer should be carefully designed because the common layer like cathode must be connected with a low resistance between adjacent pixels for luminance uniformity.

In conclusion, we believe that transient image quality without reducing system level performance such as power consumption can be improved through discussed further engineering work.

4. Conclusion

To study the effect of the lateral leakage current in the AMOLED display on the p-HTL concentration, a passive driving color panel with RGB OLEDs and a mono panel with only a single color were fabricated. We obtained an accurate OLED model by measuring the lateral sheet resistance current and mono color OLED characteristics. In addition, 1.5-in AMOLED panels based on the n-type LTPS 4T2C pixel circuit with different doping concentrations were produced. We quantitatively analyzed the luminance variation and color shift of the reddish overshoot phenomenon during the transition from black to white. This effect was effectively

reduced for p-HTL concentrations below 1%. The SPICE simulation results for the new OLED model demonstrate the reddish overshoot mechanism related to the lateral resistance of the OLED common layer, difference in turn-on voltages and capacitances among RGB OLEDs, and luminance state of the neighboring pixels.

We proposed an optimal lateral resistance value for the common organic layer for each PPI based on simulation. This study is useful for various organic electronics as well as OLED displays and presents an analysis method for studying the effect of OLED characteristics on image quality in the dynamic operation state of the AMOLED panel.

Reference

[1] T. Kohno, H. Kageyama, M. Miyamoto, M. Ishii, N. Kasai, N. Nakamura, H. Akimoto, High-speed programming architecture and image- sticking cancellation technology for high-resolution low-voltage AMOLEDs, IEEE Trans. Electron Devices, 58 (10) (2011), pp. 3444–3452, https://doi.org/10.1109/TED.2011.2162647

[2] C.W. Ko, Y.T. Tao, Bright white organic light-emitting diode, Appl. Phys. Lett. 79 (25) (2001), pp. 4234–4236, https://doi.org/10.1063/1.1425454

[3] S. Reineke, F. Lindner, G. Schwartz, N. Seidler, K. Walzer, B. Lussem, K. Leo, White organic light-emitting diodes with fluorescent tube efficiency, Nature 459 (2009), pp. 234–238, https://doi.org/10.1038/nature08003

[4] C.W. Han, J.S. Park, H.S. Choi, T.S. Kim, Y.H. Shin, H.J. Shin, M.J. Lim, B.C. Kim, H.S. Kim, Y.H. Tak, C.H. Oh, S.Y. Cha, B.C. Ahn, Advanced technologies for UHD curved OLED TV, J. Soc. Inf. Disp. 22 (11) (2015), pp. 552–563, https://doi.org/10.1002/jsid.287

[5] T. Fujii, C. Kon, Y. Motoyama, K. Shimizu, T. Shimayama, T. Yamazaki, T. Kato, S. Sakai, K. Hashikaki, K. Tanaka, Y. Nakano, 4032ppi high resolution OLED microdisplay, J. Soc. Inf. Disp. 26 (3) (2018), pp. 178-186, https://doi.org/10.1002/jsid.656

[6] J. G. Kim, J. S. Lee, H. Hwang, E. Kim, Y. Choi, J. H. Kwak, S. J. Park, Y. Hwang, K. W. Choi, Y. W. Park, B.K. Ju, Modeling of flexible light extraction structure: Improved flexibility and optical efficiency for organic light-emitting diodes, Org. Electron. 85 (2020) 105760, https://doi.org/10.1016/j.orgel.2020.105760

[7] J. Kido, M. Kimura, K. Nagai, Multilayer white light emitting organic electroluminescent device, Science 267 (5202) (1995), 1332-1334, https://doi.org/10.1126/science.267.5202.1332

[8] J. H. Kwon, RGB color patterning for AMOLED TVs, Inf. Disp. 29 (2) (2013), pp. 12-15, https://doi.org/10.1002/j.2637-496X.2013.tb00592.x

[9] C.C Chang, M.T. Hsieh, J.F. Chen, S.W. Hwang, C.H. Chen, Highly power efficient organic light-emitting diodes with a p-doping layer, Appl. Phys. Lett. 89 (25) (2006) 253504, https://doi.org/10.1063/1.2405856

[10] C. Murawki, C. Fuchs, S. Hofmann, K. Leo, M.C. Gather, Alternative p-doped hole transport material for low operating voltage and high efficiency organic light-emitting diodes, Appl. Phys. Lett. 105 (11) (2014) 113303, https://doi.org/10.1063/1.4896127

[11] X. Zhou, J. Blochwitz, M. Pfeiffer, A. Nollau, T. Fritz, K. Leo, Enhanced hole injection into amorphous hole-transport layers of organic light-emitting diodes using controlled p-type doping, Adv. Funct. Mater. 11 (4) (2001), pp. 310-314, https://doi.org/10.1002/1616-3028(200108)

[12] I. Slowik, A. Fischer, H. Frob, S. Lenk, S. Reineke, K. Leo, Novel organic light-emitting diode design for future lasing applications, Org. Electron. 48 (2017), pp. 132-137, https://doi.org/10.1016/j.orgel.2017.05.048

[13] M. Diethelm, L. Penninck, S. Altazin, R. Hiestand, C. Kirsch, B. Ruhstaller, Quantitative analysis of pixel crosstalk in AMOLED displays, J. Inf. Dis. 19 (2) (2018), pp. 61-69, https://doi.org/10.1080/15980316.2018.1428232

[14] L. Penninck, M. Diethelm, S. Altazin, R. Hiestand, C. Kirsch, B. Ruhstaller, Modeling crosstalk through common semiconductor layers in AMOLED displays, J. Soc. Inf. Disp. 26 (9) (2018), pp. 546-554, https://doi.org/10.1002/jsid.671

[15] D. Zhang, J. Qiao, D. Zhang, L. Duan, Ultrahigh efficiency green PHOLEDs with a voltage under 3V and a power efficiency of nearly 110 lmW^{-1} at luminance of 10000cdm^{-2}, Adv. Mater. 29 (40) (2017) 1702847, https://doi.org/10.1002/adma.201702847

[16] S. Katsui, H. Kobayashi, T. Nakagawa, Y. Tamatsukuri, H. Shishido, S. Uesaka, R. Yamaoka, T. Nagata, T. Aoyama, K. Nei, Y. Okazaki, T. Ikeda, S. Yamazaki, A 5291-ppi organic light emitting diode display using field effect transistors including a c-axis aligned crystalline oxide semiconductor, J. Soc. Inf. Disp. 27 (8) (2019), pp. 497-506, https://doi.org/10.1002/jsid.822

[17] P.E. Malinowski, A. Nakamura, D. Janssen, Y. Kamochi, I. Koyama, Y. Iwai, A. Stefaniuk, E. Wilenska, C.S. Redondo, D. Cheyns, S. Steudel, P. Heremans, Photolithographic patterning of organic photodetectors with a non-fluorinated photoresist system, Org. Electron. 15 (2014), pp. 2355-2359, https://doi.org/10.1016/j.orgel.2014.07.005

[18] E. Bodenstein, M. Schober, M. Hoffmann, C. Metzner, U. Vogel, Realization of RGB colors from top-emitting white OLED by electron beam patterning, J. Soc. Inf. Disp. 26 (9) (2018), pp. 555-560, https://doi.org/10.1002/jsid.674

[19] Y. Zheng, A. Fischer, N. Sergeeva, S. Reineke, S. C.B. Mannsfeld, Exploiting lateral current flow due to doped layers in semiconductor devices having crossbar electrodes, Org. Electron. 65 (2019), pp. 82-90, https://doi.org/10.1016/j.orgel.2018.10.040

[20] C. Kim, K. Kim, O. Kwon, J. Jung, J.K. Park, D.H. Kim, K. Jung, FMM Pixel Patterning for Various OLED Displays, SID Symp. Dig. Tech. Pap. 51 (1) (2020), pp. 905-908, https://doi.org/10.1002/sdtp.14017

[21] T. Kohno, H. Kageyama, M.Miyamoto, N. Nakamura, H. Akimoto, AMOLEDs with a pixel driving architecture for eliminating crosstalk, IEEE Trans. Electron Devices, 59 (11) (2012), pp. 3024–3029, https://doi.org/10.1109/TED.2012.2213256

[22] H.W. Hwang, S. Hong, S.S. Hwang, K.W. Kim, Y.M. Ha, H.J. Kim, Analysis of recoverable residual image characteristics of flexible organic light emitting diode displays

using polyimide substrates, IEEE Electron Device Lett. 40 (7) (2019), pp. 1108–1111, https://doi.org/10.1109/LED.2019.2914142

[23] H. J. Shin, S. H. Choi, J. Y. Choi, J. K. Park, S. J. Kim, S. H. Yun, J. R. Seo, S. J. Bae, H. S. Kim, C. H. Oh, A high image quality organic light-emitting diode display with motion blur reduction for ultrahigh resolution and premium TVs, J. Soc. Inf. Disp. 28 (6) (2020), pp. 557-565, https://doi.org/10.1002/jsid.919

[24] C. L. Lin, P.C. Lai, L.W. Shih, C.C. Hung, P.C. Lai, T.Y. Lin, K.H. Liu, T.H. Wang, Compensation pixel circuit to improve image quality for mobile AMOLED displays, IEEE J. Solid State Circuits, 54 (2) (2019), pp. 489-500, https://doi.org/10.1109/JSSC.2018.2881922

[25] Y.H. Jang, D.H. Kim, W. Choi, M.G. Kang, K.I. Chun, J. Jeon, Y. Ko, U. Choi, S.M. Lee, J.U. Bae, K.S. Park, S.Y. Yoon, I.B. Kang, Internal compensation type OLED display using high mobility oxide TFT, SID Symp. Dig. Tech. Pap. 48 (1) (2017), pp. 76-79, https://doi.org/10.1002/sdtp.11567

[26] J. Kim, M. Kim, J.M. Kim, S.R. Kim, S.W. Lee, Driving technology for improving motion quality of active-matrix organic light-emitting diode display, Opt. Eng. 53 (9) (2014) 093105, https://doi.org/10.1117/1.OE.53.9.093105

[27] F. Peng, H. Chen, F. Fou, Y.H. Lee, M. Wand, M.C. Li, S.L. lee, S.T. Wu, Analytical equation for the motion picture response time of display devices, J. Appl. Phys. 121 (2) (2017) 023108, https://doi.org/10.1063/1.4974006

[28] R. L. Lin, J. Y. Tsai, D. Buso, G. Zissis, OLED equivalent circuit model with temperature coefficient and intrinsic capacitor, IEEE Trans. Ind. Appl. 52 (1) (2016), pp. 493–501, https://doi.org/10.1109/TIA.2015.2464180

[29] Y. Choi, M. Kim, J. Park, H. Shin, Analysis of organic light-emitting diode SPICE models with constant or voltage-dependent components, J. Nanosci. Nanotechnol. 20 (8) (2020), pp. 4773–4777, https://doi.org/10.1166/jnn.2020.17801

[30] B. Ruhstaller, T. Flatz, M. Moos, G. Sartoris, M. Kiy, T. Beierlein, R. Kern, C. Winnewisser, R. Pretot, N. Chebotareva, P. Schaaf, Optoelectronic OLED modeling for device optimization and analysis. SID Symp. Dig. Tech. Pap. 38 (1) (2012), pp. 1686–1690 https://doi.org/10.1889/1.2785649

[31] F. Salameh, A. A. Haddad, A. Picot, L. Canale, G. Zissis, M. Chabert, P. Maussion, Modeling the luminance degradation of OLEDs using design of experiments, IEEE Trans. Ind. Appl. 55 (6) (2019), pp. 6548–6558 https://doi.org/10.1109/TIA.2019.292915

[32] M. Kim, J.M. Kim, D. Lee, S.W. Lee, Overdrive technology compensating for ambient temperature, Opt. Eng. 54(2), 023107 (2015), https://doi.org/10.1117/1.OE.54.2.023107

[33] J. Kim, M. Kim, J.M. Kim, S.R. Kim, S.W. Lee, Driving technology for improving motion quality of active-matrix organic light-emitting diode display, Opt. Eng. 53(9), 093105 (2014), https://doi.org/10.1117/1.OE.53.9.093105

[34] R. Okuda, K. Miyoshi, N. Arai, M. Tomikawa, Polyimide coatings for OLED applications, J. Photopolym. Sci. Technol. 17 (2004) 207–213. https://doi.org/10.2494/photopolymer.17.207

Analysis and simulation of reddish overshoot in active matrix organic light-emitting diode display with varying p-doped hole transport layer concentrations

Jung-Min Lee[a,b], Chang Heon Kang[b], Juhn Suk Yoo[b], Han Wook Hwang[b], Soon kwang Hong[b], Yong Min Ha[b] and Byeong-Kwon Ju[a,*]

[a] Display and Nanosystem Laboratory, Department of Electrical Engineering, Korea University, Seoul 02841, Republic of Korea

[b] LG Display Co., Ltd., Paju 10845, Gyeonggi-do, Republic of Korea

Highlights

- Passive driving OLED and AMOLED display with varying p-HTL concentration

- Effect of the lateral leakage current on the AMOLED display

- Analysis of reddish overshoot mechanism through SPICE simulations and accurate OLED modeling

- An optimal lateral resistance value for the common organic layer is proposed for each PPI

Declaration of interest Statement

☒ The authors declare that they have no known competing financial interests or personal relationships that could have appeared to influence the work reported in this paper.

☐The authors declare the following financial interests/personal relationships which may be considered as potential competing interests: